This review provides insight into the most advanced InhA inhibitors, which show clear evidence of successful target engagement and represent excellent pointers for further drug optimization.

A new 'golden age' for the antitubercular target InhA

Kaja Rožman[1], Izidor Sosič[1], Raquel Fernandez[2], Robert J. Young[3], Alfonso Mendoza[2], Stanislav Gobec[1] and Lourdes Encinas[2]

[1] Faculty of Pharmacy, University of Ljubljana, Aškerčeva 7, SI-1000 Ljubljana, Slovenia
[2] Diseases of the Developing World, Tres Cantos Medicines Development Campus, GlaxoSmithKline, Severo Ochoa 2, 28760 Tres Cantos, Madrid, Spain
[3] GlaxoSmithKline Medicines Research Centre, Stevenage, Herfordshire SG1 2NY, UK

The increasing prevalence of multidrug-resistant strains of *Mycobacterium tuberculosis* is the main contributing factor in unfavorable outcomes in the treatment of tuberculosis. Studies suggest that direct inhibitors of InhA, an enoyl-ACP-reductase, might yield promising clinical candidates that can be developed into new antitubercular drugs. In this review, we describe the application of different hit-identification strategies to InhA, which clearly illustrate the druggability of its active site through distinct binding mechanisms. We further characterize four classes of InhA inhibitors that show novel binding modes, and provide evidence of their successful target engagement as well as their *in vivo* activity.

Introduction

Tuberculosis (TB) is caused by *Mycobacterium tuberculosis*, and it remains the most deadly infectious disease in the world, responsible for the death of ~1.5 million people every year. Although TB incidence and mortality rate have been greatly reduced over the years, this progress is mostly overlooked owing to the increasing prevalence of multidrug-resistant TB (MDR-TB) and extensively drug-resistant TB (XDR-TB). These resistant strains of TB fail to respond to standard antibiotic treatments [in particular isoniazid (isonicotinic acid hydrazide; INH) and rifampicin], and they are therefore a cause for great concern among medical workers worldwide [1,2]. Another highly important contemporary challenge is co-infection with HIV and TB, which is a leading cause of death among people who are HIV positive [3].

The majority of TB cases are treatable. However, with the current long and complex regimen of drugs [4] this can lead to lack of adherence owing to adverse side effects, thus providing suboptimal treatment responses. Although numerous attempts have been made to shorten the duration of therapy of drug-susceptible TB and to improve the outcomes for MDR-TB treatments, the number of deaths is still high [5]. Therefore, there is an urgent need to develop

Corresponding author: Gobec, S. (stanislav.gobec@ffa.uni-lj.si), Encinas, L. (lourdes.p.encinas-prieto@gsk.com)

Lourdes Encinas graduated with a degree in chemistry from the University of Basque Country in 2003 and received her PhD in chemistry from the Autonoma University of Madrid in 2008, under the supervision of Dr Chiara at CSIC (Madrid). Her thesis dealt with the development of new methods for solution-phase synthesis of oligosaccharides using supported and chemically tagged reagents. She subsequently joined GSK to work on the development of new drugs against tuberculosis. She has been involved in several projects – target-based and phenotypic – in collaborations like ORCHID, a consortium funded by the EU. Her main interests include drug discovery and neglected diseases.

Stanislav Gobec is professor of pharmaceutical chemistry at the Faculty of Pharmacy, University of Ljubljana. His research interests are structure-based *in silico* design, synthesis and evaluation of small-molecule enzyme inhibitors for different therapeutic areas. He has authored more than 150 papers and book chapters, and has been involved in EU-funded antibacterial drug discovery programs.

Kaja Rožman is a PhD student at the Faculty of Pharmacy, University of Ljubljana, Slovenia, under the supervision of Professor Stanislav Gobec. She studied pharmacy at the Faculty of Pharmacy in Ljubljana, and graduated in 2014. Her master's thesis was on Toll-like receptor 4 (TLR4) and the design of its antagonists. She is currently working in the field of antibacterial drug design, with the main focus on targeting bacterial cell wall biosynthesis.

http://dx.doi.org/10.1016/j.drudis.2016.09.009

new antitubercular drugs with novel chemical scaffolds that have distinctive inhibitory binding modes and/or new mechanisms of action.

A significant barrier in the delivery of TB drugs to their site of action is the very complex and poorly permeable cell envelope of mycobacteria. Mycolic acids are α-branched, β-hydroxylated fatty acids with chains of 60–90 carbon atoms in length, and they are major and essential components of the mycobacterial cell envelope. Their biosynthesis is controlled by two elongation systems: fatty acid synthase type I (FAS-I) and fatty acid synthase type II (FAS-II). The FAS-II enzymes are viable targets for drug development, because eukaryotic cells only use a FAS-I enzyme to synthesize fatty acids. InhA is an enoyl-acyl carrier protein (ACP) reductase of the FAS-II system, and it catalyzes NADH-dependent reduction of the double bond at position two of growing fatty acid chains that are linked to ACP [6,7]. The first crystal structure of InhA was published in 1995, and it has subsequently been a much investigated target in antitubercular drug discovery [8]. Indeed, based on the success of INH in treating patients with TB, InhA is a clinically validated target.

INH was discovered in 1952, and has been widely used as an anti-TB therapy ever since [9]. INH is a prodrug that is transformed *in vivo* by the mycobacterial catalase-peroxidase enzyme KatG into the reactive isonicotinyl acyl radical, which can then form a covalent adduct with the nicotinamide adenine dinucleotide cofactor of InhA (INH-NAD adduct) [6]. Interestingly, the dependency on KatG activation for INH-mediated killing is also the source of the main clinical weakness associated with the use of INH, because 40–95% of INH-resistant *M. tuberculosis* clinical isolates have mutations in *katG* that lead to impaired activation of INH [10,11]. Although mutations in the InhA promoter region are also detected in clinical isolates, these only produce low-level resistance to INH. Taken together, these observations suggest that direct inhibitors of InhA that do not require KatG activation would be promising candidates for targeting INH-resistant *M. tuberculosis* strains [12,13].

Different classes of direct InhA inhibitors have been discovered. However, progression of these toward the clinic has been limited. This has occurred for a variety of reasons, which include a tendency for potent enzymatic inhibition not translating into whole-cell activity, a narrow therapeutic selectivity window and/or poor pharmacokinetic properties. The chemical diversity of InhA inhibitors reported in patent applications [14] and publications [15–18] has been reviewed over the past 5 years. Therefore, the present review focuses on recent progress in the discovery of InhA inhibitors that has been fueled by property-guided design, up-to-date screening practices and knowledge obtained from co-crystal structures that have been reported for InhA with its ligands. In particular, our main goal was to highlight InhA inhibitors that have novel binding modes, show solid evidence of successful target engagement and have *in vivo* activity in murine models of TB. These are classified into four groups: triclosan derivatives, pyridomycin, 4-hydroxy-2-pyridones and thiadiazoles.

Screening technologies

InhA is a clinically validated anti-TB drug discovery target that appears to be readily druggable by a broad structural variety of inhibitors. Different classes of direct InhA inhibitors have been identified using HTS. Additionally, encoded library technology, fragment-based screening and *in silico* design strategies have been exploited.

HTS

HTS is the process of testing a large number of diverse chemical structures against defined proteins as disease targets (target-based HTS), or by phenotypic screening, to identify hit compounds. Compared with traditional drug screening methods, HTS is characterized by its simplicity, speed, low cost and high efficiency. It can usually provide high-quality information about ligand–target interactions [19]. The initial expectations from HTS were that a drug would be derived directly from the screening; however, in reality, such screening hits simply represent chemical starting points that need to be optimized, just as for any other drug discovery approach [20]. An additional drawback of target-based HTS in antibacterial drug discovery could be discrepancy between IC_{50} and minimum inhibitory concentration (MIC) values owing to poor inhibitor penetration, leading to suboptimal starting points for further development.

Different HTS campaigns have been carried out using InhA as a target. The first HTS for InhA led to the identification of piperazine indoleformamides (Fig. 1a) and pyrazoles (Fig. 1b) as novel leads in the development of InhA inhibitors [21,22]. Later, HTS carried out by He *et al.* [23] identified 30 hits that inhibited InhA and did not affect the activity of the FabI enzymes from *Escherichia coli* or *Plasmodium falciparum*. Of these, pyrrolidine carboxamides (Fig. 1c) were chosen as lead compounds for further optimization. An arylamide series, of which the general structure is shown in Fig. 1d, was the largest series of compounds identified. Optimization primarily focused on the A and B rings here [24]. Unfortunately, owing to different factors like poor penetration (caused by low membrane permeability, efflux and/or detoxification effects) most of these series of compounds suffered from poor antibacterial activity and did not yield any potent InhA inhibitors that are effective against *M. tuberculosis* [15]. The imidazopiperidines (Fig. 1e) were discovered by Wall *et al.* [25] as a potential class of InhA inhibitors, although these also failed as potential antitubercular agents owing to lack of correlation between IC_{50} values and MICs.

However, owing to the attractiveness of this target, screening campaigns continued and novel hits with inhibitory potencies against InhA that were <10 μM were then identified. Two thiadiazoles were the best compounds obtained at this stage (Fig. 1f, compounds **1**,**2**), both of which showed activity against *M. tuberculosis* InhA in the nanomolar range, along with a good therapeutic window *in vitro*. A significant shift in the MICs in strains overexpressing the target was indicative that these antitubercular activities were mainly mediated by InhA inhibition. Further efforts were focused on optimizing the *in vivo* properties of these lead compounds, with an emphasis on the chemical properties that affect their ADME and the factors that affect their antibacterial activities, such as their uptake, efflux and detoxification mechanisms. As a result, thiadiazole **3** (Table 1) was identified as a promising candidate that had *in vivo* activity similar to INH at equivalent free exposure [26]. Another successful example of HTS technology was recently published, where the identification of a new class of direct InhA inhibitor, the 4-hydroxy-2-pyridones, was

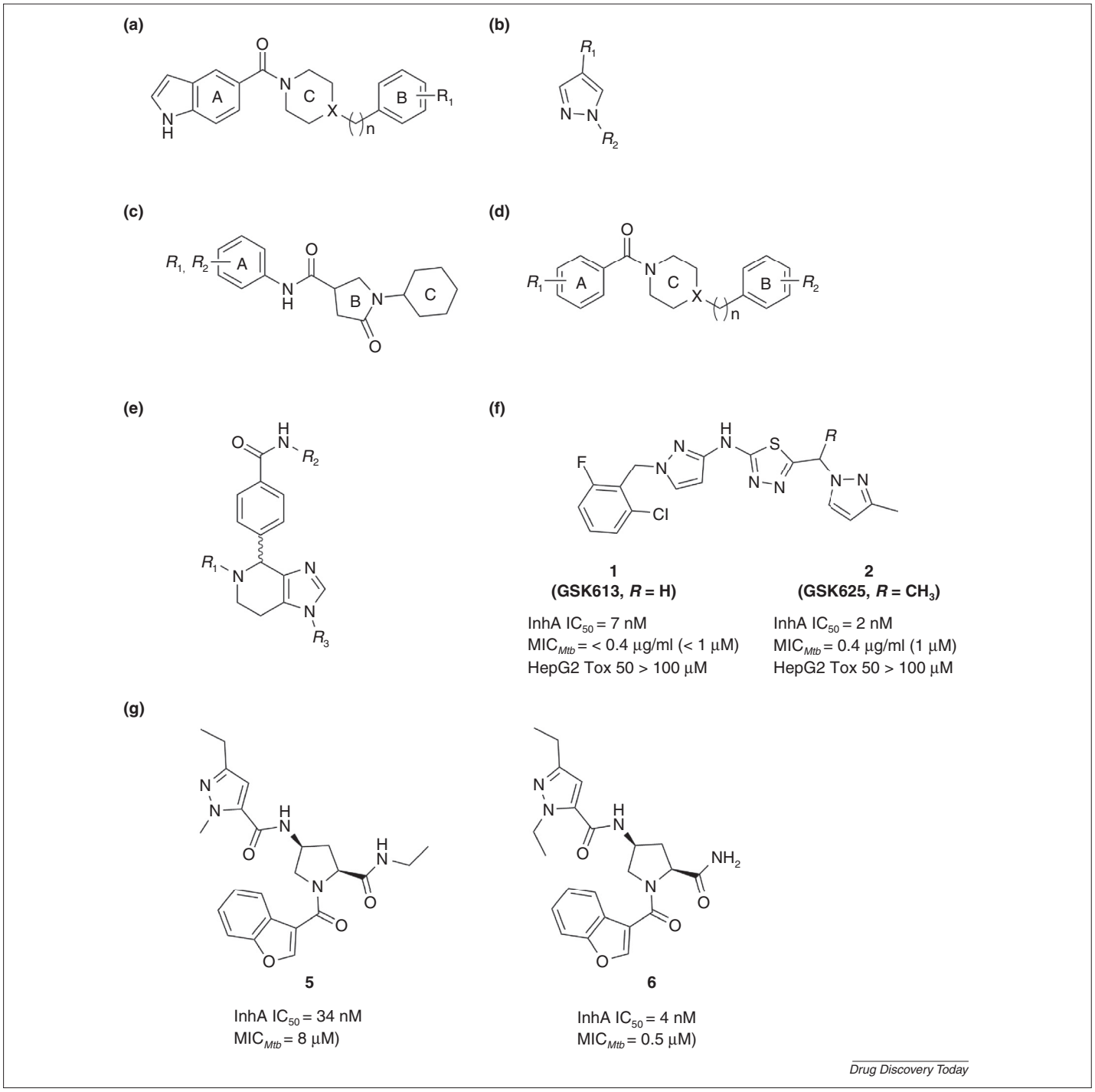

FIGURE 1

General structures of InhA inhibitors identified in HTS campaigns [21–25,29]: **(a)** piperazine indoleformamides, **(b)** pyrazoles, **(c)** pyrrolidine carboxamides, **(d)** arylamides, **(e)** imidazopiperidines, **(f)** thiadiazoles, **(g)** proline series.

reported using phenotypic HTS [27]. Compound **4** (Fig. 2) is a promising small-molecule InhA inhibitor.

Encoded library technology

Encoded library technology was first proposed in the 1990s by Brenner and Lerner [28] as a technology platform that uses DNA-tagged combinatorial libraries to identify small-molecule compounds that bind to protein targets. Each molecule in the encoded library comprises a unique combination of building blocks that are attached to a dsDNA coding region, whereby each cycle of synthetic chemistry is encoded by ligation of a short DNA tag that identifies the building block added. Using split-and-mix techniques, multibillion-membered libraries can be readily constructed. The libraries are screened by affinity-driven selection. Finally, binder deconvolution by sequencing of the DNA tags and hit confirmation by off-DNA re-synthesis are required. The modest material consumption allows multiple selection conditions to be tested in parallel.

TABLE 1

Structure and properties of optimized lead compound 3 [26]

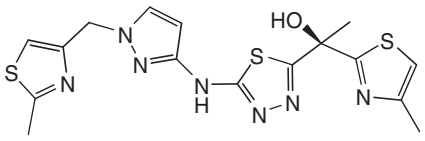

3
(GSK693)

Physicochemical properties	Molecular weight	419.6 g/mol
	Clog *P*[a]	0.71
	Artificial membrane permeability	1.9×10^{-5} cm/s
	Solubility CLND[b]	413 μM
Activity profile	InhA IC_{50}	7 nM
	Mtb MIC	0.2 μM
	Mtb intracellular MIC	0.2 μM
Cytochrome P450 profile	CYP3A4 VR assay IC_{50} [c]	>50.1 μM
	CYP3A4 VG assay IC_{50} [d]	25.1 μM
Cytotoxicity profile	HepG2 cytotoxicity (Tox 50)[e]	>50 μM
	Cell health (membrane, nucleus, mitochondria)	>199.5 μM
Genetic toxicity	Ames test	Negative
Cardiovascular profile	QPatch IC_{50}	>50 μM
***In vitro* metabolic stability (microsomes)**	Cli mouse[f]	2.1 ml/min/g
	Cli human	0.2 ml/min/g
***In vivo* pharmacokinetic study in mice**	Cl (4 mg/kg iv)	83 ml/min/kg
	Vss[g] (4 mg/kg iv)	2.58 l/kg
	$t_{1/2}$ [h] (4 mg/kg iv)	0.94 h
	T_{max} [i] (100 mg/kg po)	0.42 h
	C_{max} [j] (100 mg/kg po)	37,271 ng/ml
	DNAUC[k]	798.6 ng/h/ml per mg/kg

[a] Clog *P*, fragment-based prediction of logarithm of partition coefficient [53].
[b] CLND, chemiluminescent nitrogen detection, solubility values within 85% of maximum possible concentration (as determined from DMSO stock concentration).
[c] CYP3A4 VR assay, dealkylation of Vivid™ Red to yield resorufin.
[d] CYP3A4 VG assay, dealkylation of Vivid™ Green to yield rhodamine.
[e] HepG2 cytotoxicity (Tox 50), cytotoxicity on human liver cancer cell line; dose at which toxicity occurs in 50% of cases (Tox 50).
[f] Cl, clearance.
[g] Vss, volume of distribution at steady-state.
[h] $t_{1/2}$, half-life of a drug.
[i] T_{max}, the time needed for a drug to reach the maximum plasma concentration after its administration.
[j] C_{max}, maximum serum concentration of the drug after its administration.
[k] DNAUC, oral dose-normalized area under the curve.

The identification of a novel series of InhA inhibitors by encoded library technology and their subsequent optimization was described by Encinas *et al.* [29]. In their study, selections were conducted in parallel against a panel of DNA-encoded libraries, under conditions of protein alone, protein with NAD^+ and protein with NADH. Enrichment of specific structures was particularly evident for selections run in the presence of the NADH cofactor. A putative hit with an amino-proline scaffold was re-synthesized off-DNA, and was considered as a suitable starting point for further medicinal chemistry optimization (Fig. 1g, compound **5**). The proline series was chemically distinct from previously reported series, although its binding took place on the same site as the thiadiazole series. The SAR around the compound **5** hit were fairly narrow, although some improvements in inhibitory potency and other properties were achieved, which resulted in the synthesis of the optimized lead compound **6** (Fig. 1g). Despite a good balance between inhibition of InhA and antitubercular potency, compound **6** was inactive in a murine TB acute-infection model, for reasons that still remain unclear [29]. However, this study by Encinas *et al.* [29] demonstrated that encoded library technology is a suitable platform for the identification of potent InhA inhibitors.

Fragment-based screening

Fragment-based drug discovery has seen widespread uptake and tangible progress over the past decade, and it is particularly interesting for academic screening [30], because a small library of compounds enables widespread sampling of potential interactions (for review, see [31]). This technique requires deep knowledge of the target (e.g. sensitive biochemical and/or biophysical assays to identify the hits, followed by X-ray-guided design to improve the activity) to improve the activity of initial hits while maintaining good physical properties. To date, no data have been published on InhA inhibitors discovered in this way; however campaigns are in progress through strategic alliances [32].

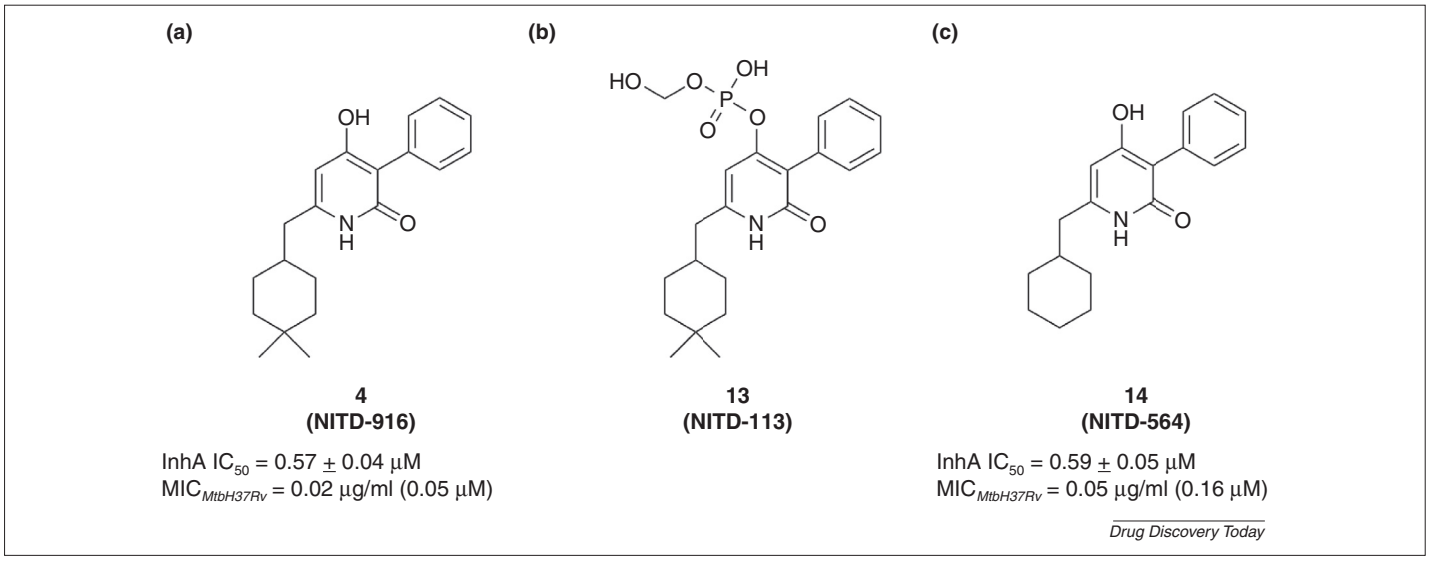

FIGURE 2

Chemical structures of potent 4-hydroxy-2-pyridone inhibitors of InhA [27]. **(a)** Compound **4**, **(b)** compound **13** and **(c)** compound **14**.

InhA inhibitors

Triclosan derivatives

Triclosan (Fig. 3a) has broad-spectrum antimicrobial activity, although it has a limited therapeutic window following intravenous administration. Despite its relatively modest antimycobacterial activity (MIC = 12.5 μg/ml), it is still considered an attractive lead for further optimization [33,34]. Triclosan is a reversible inhibitor of FabI from *E. coli*, and an inhibitor of InhA, where it binds preferably to the enzyme–NAD^+ complex (K_i = 0.2 μM). In this complex, the phenolic hydroxyl group of triclosan interacts with the hydroxyl group of Tyr158 [35]. Several analogs have been synthesized, which have been reported in previous reviews [15,16,18]. One of the most recent derivatives is the slow, tight-binding inhibitor **7** (Fig. 3b). This inhibitor forms additional hydrophobic interactions with amino acids Ala198, Met199, Ile202 and Val203 of InhA in the substrate-binding loop (PDB ID: 2X22, 2X23) (Fig. 3b) [34], which contribute to the >400-fold higher affinity of **7** for the enzyme–cofactor complex (K_i = 22 pM; IC_{50} = 50.7 ± 4 nM) when compared with the parent compound **8** (Fig. 3c) [36]. Following the previously reported lack of efficacy of InhA inhibitors, **7** was evaluated for efficacy when administered via an intraperitoneal route in a rapid animal model of TB infection [37]. Compared with untreated controls, **7** did not reduce the bacterial load in the lung, although it significantly reduced the bacterial counts in the spleen (by 0.57 ± 0.26 $\log_{10}$ units; P = 0.007), which is an important secondary site of TB infection. Pan *et al.* [38] concluded that the data from this animal model of TB infection indicate that the slow-onset kinetics, which affect the residence time of compound **7** on InhA (24 min), have a positive impact on the *in vivo* efficacy (MIC = 3.125 μg/ml).

The concept of improving the *in vivo* efficacy by slow-onset InhA inhibition was further investigated by Li *et al.* [39], who reported that helix-6 within the substrate-binding loop of InhA adopts a closed conformation after local refolding during the slow, two-step conversion of EI to EI*, which is caused by induced-fit inhibition of InhA. Based on these data, Li *et al.* constructed computational models of the EI to EI* transition state during loop isomerization, which provided information about specific interactions that are crucial to modulation of the energy barrier to inhibitor binding. They showed that adding a bulky group to the ligand (i.e. compound **9**; PDB ID: 5CPF; Fig. 3b) negated the effect of alanine mutation (I215A) and increased the energy barrier to ligand dissociation, thus promoting longer residence time of the inhibitor. Newly obtained insights into specific ligand–protein interactions and how these might control the induced-fit kinetics should prove very useful for further optimization of such InhA inhibitors [40]. Recently, it was discovered that, despite the rapid distribution of compound **7** to the major organs in mice and baboons, it had no impact on the bacterial load in the lungs of mice – the primary site of infection [41].

A separate study investigated another series of triclosan derivatives with modifications at positions 5 and 4′ (Fig. 3a) [42]. Of their 27 derivatives, seven showed improved potency in comparison with triclosan. Closer analysis of the SAR showed that substitution of chlorine at position 5 with cyano or a bulkier triazole group retained or increased the potency of these triclosan analogs. However, addition of a 4-phenyl group to the triazole ring resulted in complete loss of activity. This indicates possible size limitation within the binding pocket. Conversely, an additional *n*-butyl chain at position 4 of the triazole ring led to the most active derivative of this series: compound **10** (IC_{50} = 90 nM; Fig. 3d). The antimycobacterial activity of compound **10** was ~20-fold greater than that of triclosan (MICs = 0.6 and 12.5 μg/ml, respectively). Stec *et al.* [42] also evaluated compound **10** and other active compounds of this series against *M. tuberculosis* strains that are resistant to INH because of mutations in *katG* ($mc^2$4977 and $mc^2$5855); and, furthermore, the *M. tuberculosis* strain overexpressing *inhA* ($mc^2$4914) was resistant to **10**, supporting the fact that these analogs engage with InhA to produce their antimycobacterial effects. Unfortunately, **10** has very low oral bioavailability, which appears to be due to its poor water solubility and rapid phase II metabolism. Even though all

(a)

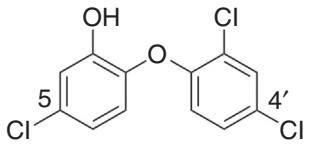

Triclosan

IC_{50} = 1000 ± 100 nM

$MIC_{MtbH37Rv}$ = 12.5 ± 0 μg/ml

(b)

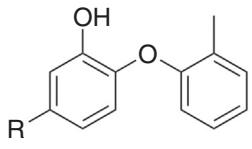

7

(**PT70**: R = $(CH_2)_5CH_3$)

IC_{50} = 50.7 ± 4 nM

$MIC_{MtbH37Rv}$ = 3.125 μg/ml

9

(**PT163**: R= 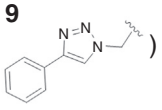)

(c)

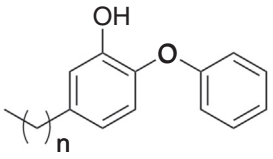

8

(**6PP**: n = 5)

IC_{50} = 11 ± 1 nM

$MIC_{MtbH37Rv}$ = 2.1 ± 0.9 μg/ml

(d)

Compound	Antimycobacterial activity, MIC (μg/ml)		Enzyme inhibitory potency	Cytotoxicity
	Mycobacterium tuberculosis H37RV	*M. tuberculosis* mc²4914[a]	InhA inhibition[b] (%)	Vero cells IC_{50}, (μg/ml) and SI[c]
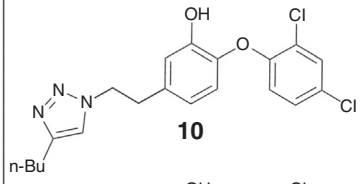 **10**	0.6 (1.5 μM)	> 80	98 ± 0.22	1–2 (SI = 1.7–3.3)
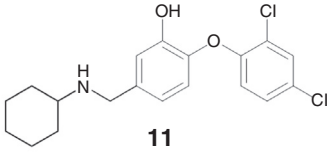 **11**	6.25 (17 μM)	12.5	39 ± 0.67	4 (SI = 0.6)
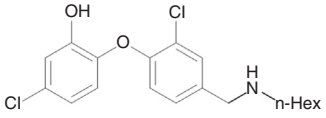 **12**	5 (14 μM)	10	38 ± 0.15	8 (SI = 1.6)
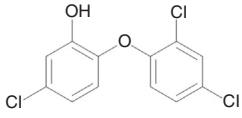 **Triclosan**	12.5 (43 μM)	20	96 ± 0.65	< 12.5 (SI < 1)

[a] An *M. tuberculosis* strain that overexpresses inhA.

[b] % Inhibition of recombinant InhA at the respective compound's MIC against *M. tuberculosis* H37Rv.

[c] Selectivity index, SI calculated as IC50 (Vero cells)/MIC (*M. tuberculosis* H37Rv).

Drug Discovery Today

FIGURE 3

(a–c) Chemical structures of triclosan **(a)** and compounds **7** and **9 (b)**, and **8 (c)** [40,43]. **(d)** Chemical structures and activities of the best triclosan-based inhibitors of InhA, compounds **10–12** [42].

of these analogs inhibited mycolic acid biosynthesis and compounds **11** and **12** affected fatty-acid methyl-ester biosynthesis, they also had low selectivity between their impact on viability of eukaryotic Vero cells and their activity against *M. tuberculosis*. Therefore, any further optimization of this compound class would need to produce more-selective compounds with better physical characteristics, to improve the pharmacokinetic exposure [42].

Pyridomycin

In the world of antimicrobial agents, natural products represent a broad and diverse set of compounds that can be suitable as therapeutics or leads for drug discovery. In this context, Hartkoorn *et al.* [44] identified InhA as a primary target for pyridomycin (Fig. 4) – a compound produced by the bacterium *Dactylosporangium fulvum*. In a series of genetic experiments, they demonstrated that pyridomycin acts as a direct competitive inhibitor of the NADH-binding site of InhA (K_i = 6.5 μM); consequently this binding site was proposed as a new druggable pocket within the InhA active site. In 2014, the co-crystal structure confirmed that pyridomycin binds in the NADH-binding site, and also that it interacts with residues in the substrate-binding pocket (PDB ID: 4BGE) [45]. This natural inhibitor showed good cell-growth inhibition (MIC = 0.31–0.63 μg/ml), and promising bactericidal potency against *M. tuberculosis* H37Rv (minimum bactericidal concentration = 0.62–1.25 μg/ml). Pyridomycin promoted a concentration-dependent reduction in mycolic acid synthesis, and it did not have any effects on the overall fatty acid content. Moreover, the cytotoxicity profile of pyridomycin was measured against two different human cell lines, where there was a 100-fold difference between *M. tuberculosis* activity and human cell cytotoxicity (EC_{50} = 50–100 μg/ml), thus excluding the possibility of its nonselective action. Analysis of the drug susceptibility of clinically relevant *M. tuberculosis* strains showed that those carrying the *katG* mutation were not resistant to pyridomycin, in contrast to what was seen for INH. However, the mutation on the *inhA* promoter resulted in increased resistance to pyridomycin and INH [44]. These observations indicated that pyridomycin represents a promising starting point for the development of compounds that can be used in the treatment of INH-resistant tuberculosis.

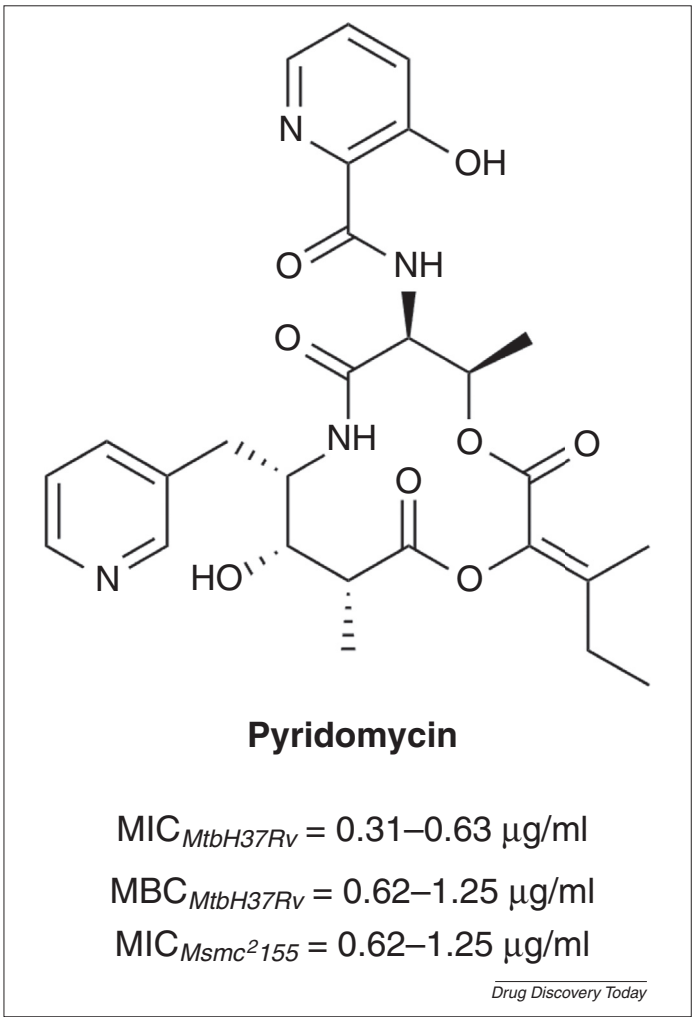

FIGURE 4

Chemical structure and antimycobacterial activities of pyridomycin [44].

4-Hydroxy-2-pyridones

Recently, a new class of direct InhA inhibitors, the 4-hydroxy-2-pyridones, was discovered using phenotypic HTS against *M. tuberculosis* H37Ra [27,46]. A small series of orally active compounds with potent bactericidal activity against several INH-resistant TB clinical isolates was identified that showed no activity against Gram-positive and Gram-negative bacterial strains. Isothermal titration calorimetry studies revealed that these 4-hydroxy-2-pyridones specifically inhibited InhA in an NADH-dependent manner, and that they partially blocked the enoyl-substrate-binding site, as evident from the co-crystal structures (PDB IDs: 4R9R, 4R9S). The most promising compound of this series, compound **4** (InhA IC_{50} = 0.57 ± 0.04 μM; Fig. 2a), was active against seven MDR-TB clinical isolates, with MIC_{99} values from 0.01 μg/ml to 0.39 μg/ml (0.04–1.25 μM), depending on the MDR-TB strain. Three of the MDR-TB clinical isolates contained a mutation in *katG* and were fully sensitive to 4-hydroxy-2-pyridones. The only clinical isolate with mutation in InhA:I194T was resistant not only to INH but also to 4-hydroxy-2-pyridones. Compound **4** showed good oral bioavailability in mice (66% at 25 mg/kg), with low systemic clearance and modest volume of distribution. Furthermore, **4** showed dose-dependent *in vivo* efficacy when orally administered (100 mg/kg once daily for 4 weeks) in an acute mouse model, which was comparable to the efficacy of rifampicin (100 mg/kg) and ethambutol (10 mg/kg), but higher than for INH (25 mg/kg). However, the major concerns for compound **4** were its high plasma-protein binding, low lung:plasma ratio and low aqueous solubility. To address these shortcomings, phosphate ester prodrug **13** (Fig. 2b) was synthesized, which resulted in a two orders of magnitude increase in its aqueous solubility. The crystal structures of InhA in complex with NADH and **4** (PDB ID: 4R9S) and **14** (PDB ID: 4R9R; Fig. 2c) showed the same position of these compounds in the active site, and provided a rationale for the NADH dependency. Five key interactions were identified, which included multiple H-bonds with cofactor NADH and Tyr158, π-stacking with the pyridine ring of NADH and hydrophobic contacts between the dimethyl-cyclohexyl and cyclohexyl moieties of **4** and **14**, respectively, within the large hydrophobic pocket. The preliminary SAR studies were expanded into a larger series of 4-hydroxy-2-pyridones, and the data here suggested that this new chemical scaffold offers great potential for further optimization to improve *in vitro* and *in vivo* potencies [27,47].

Thiadiazoles

Thiadiazole-based InhA inhibitors were initially discovered using HTS [48,49]. The lead compound **15** (Fig. 5a) was shown to be a direct, reversible inhibitor of InhA (IC_{50} = 4 nM) with good potency against *M. tuberculosis* (MIC = 0.2 μM). Structural studies

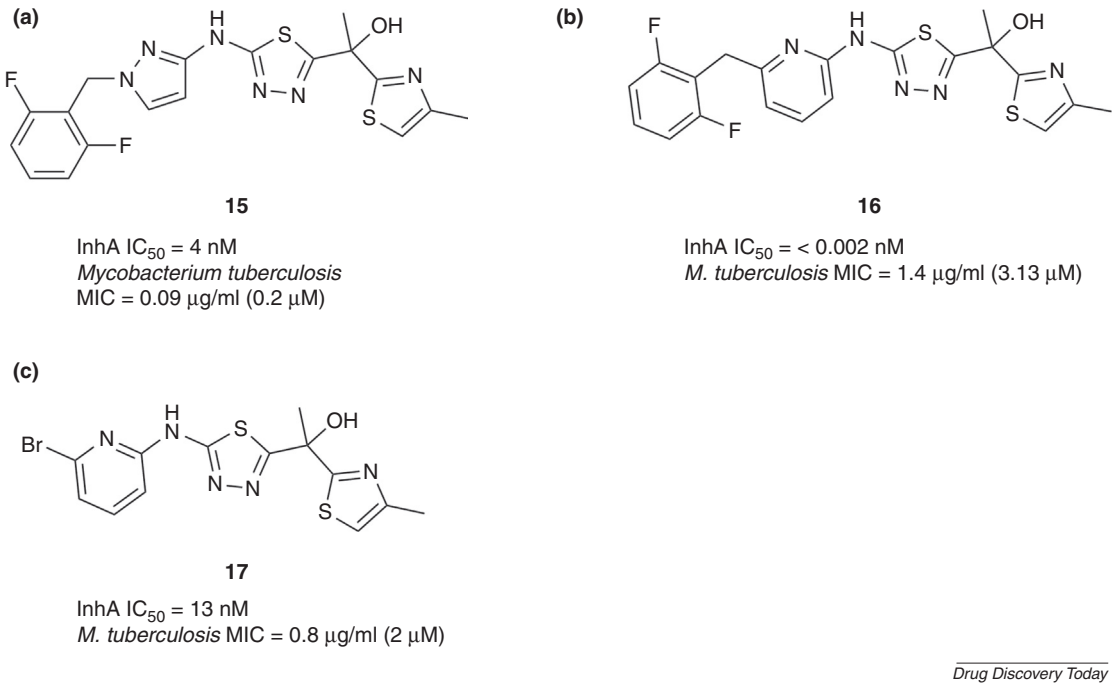

FIGURE 5

Methylthiazoles as potent inhibitors of InhA [48,50,51]. **(a)** Lead compound 15, **(b)** analog 16 of compound 15, (c) rings modified at opposite end from thiadiazole and thiazole resulted in 17.

indicated interesting observations pertinent to this structure-based drug design, including several contacts with NADH [48,49]. Based on these patent publications [48,49], a further series of methylthiazole derivatives was described (with the best of the series as **16**; Fig. 5b) [50], with evidence for tight binding of these compounds with the NADH-bound form of InhA (compound **15**, K_d = 13.7 nM). By contrast, binding of the compounds in both of these series to the NAD^+-bound form of InhA was much weaker (compound **15**, K_d = 9300 nM). These compounds demonstrated a novel mechanism of InhA inhibition, which has been described as the 'Tyr158-out' inhibitor-bound conformation of the enzyme that accommodates a neutral thiazole ring (PDB IDs: 4BQP, 4BQR). The improved activity of these compounds was rationalized by additional hydrophilic interactions with the catalytic side chain of Met98, which contributes to their more-favorable physiochemical properties. This novel binding mode is further described below.

An extension of the work on this interesting chemical scaffold by Šink *et al.* [51] explored a series of 23 potent tricyclic InhA inhibitors that were synthesized as truncates of the potent tetracyclic methylthiazole **15** (PDB ID: 4BQP). These tricyclic derivatives retained the thiadiazole and thiazole rings, and explored alterations to the other end of the molecule. Compound **17** was the most potent of this series (IC_{50} = 13 nM; MIC = 0.8 μg/ml or 2 μM; Fig. 5c), and it showed promising physical properties (Chrom log $D_{pH7.4}$ = 3.93) with good ligand efficiency (0.49 kcal/mol/atom) and ligand lipophilicity efficiency (6.63), which compared favorably to compound **15** (ligand efficiency = 0.40 kcal/mol/atom; ligand lipophilicity efficiency = 6.24). The *S*-enantiomer was shown to be the eutomer (IC_{50} = 43 nM; MIC = 0.2 μg/ml), whereas the *R*-enantiomer showed >200-fold lower potency (IC_{50} > 1 μM). Despite the good intracellular antimicrobial activity in THP-1 cells, the activity of (*S*)-**17** in the *in vivo* mouse model was weaker than INH [51].

Data on a more advanced thiadiazole **3** (Table 1) was recently published [26]. Compound **3** is a selective and bactericidal compound that is active against MDR and XDR *M. tuberculosis* clinical isolates, and orally active in murine models of TB [26]. The oral efficacy of **3** was evaluated in an acute murine model as previously described [52], at doses of 30, 100 and 300 mg/kg once daily for 7 days, using 30 mg/kg moxifloxacin as the positive control. Compound **3** showed a clear dose–response relationship, with pharmacological effects within this dose range. In mice treated with 100 mg/kg **3**, the bacterial load was reduced by 4.0 $\log_{10}$ colony-forming units per lung, which matched the reduction obtained with 30 mg/kg moxifloxacin. Compound **3** was further evaluated in an established model of TB infection at a daily dose of 300 mg/kg as a suspension in 1% methylcellulose. After 2 months of treatment of chronically infected mice, 300 mg/kg **3** and 25 mg/kg INH showed clear efficacy in terms of significant clearance of bacilli compared with the controls ($P < 0.001$). Furthermore, the differences between the treated groups were not significant, which confirmed that a direct inhibitor of InhA can retain the desirable antimycobacterial profile of INH without relying on KatG activation, thus circumventing the key INH-associated resistance problems.

Crystallography and structure-guided design

The reported complexes of various ligands with InhA have provided key insights into the enzyme mechanisms and ternary product structures. This structural information with bound substrates and structurally diverse inhibitors has defined a number of features of

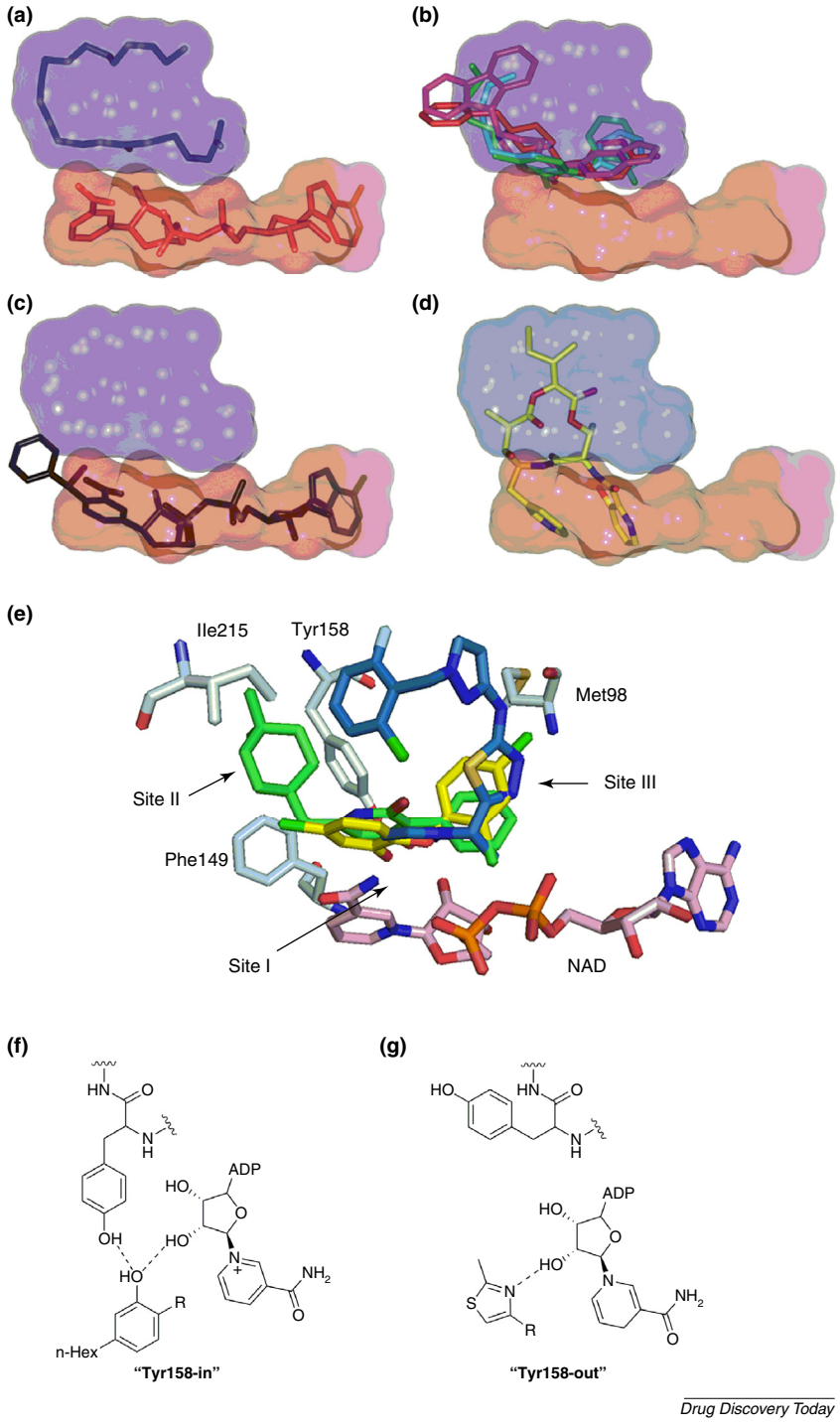

FIGURE 6

Comparison of the binding of various InhA inhibitors to the InhA binding sites. **(a)** NADH (red sticks) in the NADH-binding site (red surface) and the *trans*-2-hexadecanoyl-*N*-acetyl cysteamine thioester substrate (blue sticks) in the substrate-binding site (blue surface) (PDB ID: 1BVR9). **(b)** Triclosan derivative 5-pentyl-2-phenoxyphenol (cyan; PDB ID: 2B36), 5-(4-(9H-fluoren-9-yl)piperazin-1-yl)carbonyl-1H-indole (magenta; PDB ID: 1P44), *N*-(4-methylbenzoyl)-4-benzylpiperidine (red; PDB ID: 2NSD14) and 5-hexyl-2-(2-methylphenoxy)phenol (green; PDB ID: 2X22). **(c)** INH-NAD adduct of INH (black; PDB ID: 2IEB24). **(d)** Pyridomycin (yellow, PDB ID: 4BGE). (a–d) Modified, with permission, from [45]. **(e)** Three regions within the substrate-binding sites of InhA with overlaid protein complexes with triclosan (yellow, PBD ID: 2B35) [34], 4-hydroxy-2-pyridone 4 (green, PDB ID: 4R9S) [27] and a representative thiadiazole GSK625 (blue, PDB ID: 5JFO) [26]: site I, catalytic site; site II, hydrophobic pocket; site III, size-limited region. Carbon atoms of M98, F149, Y158 and I215 from InhA are cyan, and carbon atoms of NAD are pink. **(f)** Schematic representation of InhA catalytic site I interactions in 'Tyr158-in' and 'Tyr158-out' forms. Tyr158-in binding mode of triclosan-based derivative 7 (PT70). **(g)** Tyr158-out binding mode of methyl-thiazole derivative 15 [50].

InhA. First, in almost every case, the inhibitors bind to InhA in the presence of the NADH cofactor in either the oxidized or reduced form. A special case is seen for INH, which binds as a covalent adduct of the cofactor. By contrast, pyridomycin showed a unique mode of InhA inhibition by simultaneously forming interactions with NADH and the lipid-binding pockets of InhA. Indeed, most of the efforts to identify new direct inhibitors of InhA largely led to inhibition of the lipid–substrate binding. The elucidation of the pyridomycin-binding site offers possibilities for focused searches and rational design for small-molecule inhibitors that can bind to this region [45]. Hartkoorn *et al.* [45] compared the binding modes of various InhA inhibitors (Fig. 6a–d), which provided helpful visualization of the binding pockets.

Secondly, Shirude *et al.* [50] showed that the InhA substrate-binding site occupied by substrate-competitive inhibitors can be divided into three regions, as presented in Fig. 6e. For 'site I' the ligand interacts with the nicotinamide ring and the ribose hydroxyl group of NADH. Interestingly, compounds **2** [26], **5** [29] and **15** [50] were the first identified InhA inhibitors that did not have an oxygen atom for the interaction with the hydroxyl groups of ribose and Tyr158, which had been described for all previously reported substrate-competitive inhibitors. Furthermore, a hydrophobic 'site II' accommodates the growing alkyl chains during the catalytic reaction [54]. The intrinsic flexibility observed in this region is consistent with the requirement that the binding site accommodates chains of varying lengths. Although binding to this pocket improved the potency of some inhibitors, it usually contributed to their increased lipophilicity. Finally, for 'site III', the inhibitor forms hydrophilic contacts with Met98 or positions its hydroxyl group adjacent to the phosphate groups of NADH. In the future, further knowledge about these three regions of InhA-binding sites needs to be obtained for modulation of the physicochemical properties of InhA inhibitors.

Thirdly, the relative position of Tyr158 in the InhA catalytic site is an important structural discriminator. The interaction with Tyr158 has been described as the closed/'flipped in'/'Tyr158-in' conformation, where the phenolic oxygen of Tyr158 is oriented toward the inhibitor, and the open/'flipped out'/'Tyr158-out' conformation where Tyr158 is oriented away, as illustrated in Fig. 6f,g [50]. In contrast to the Tyr158-in inhibitors of InhA, such as pyrrolidine carboxamides, triclosan and 4-hydroxy-2-pyridones, with these various classes of Tyr158-out inhibitors Tyr158 does not form any H-bonds (i.e. proline series [29], thiadiazoles [26]) but forms van der Waals interactions. Additionally, in the thiadiazole-based series [26,50], the methyl-thiazole group interacts with the nicotinamide and ribose groups of the NADH cofactor, whereas the pyrazole 2-nitrogen forms a H-bond with the 2′-hydroxyl group of NADH. Additionally, the methyl group of the methyl thiazoles forces Tyr158 to adopt an alternative $\chi 1$ torsion angle, which is similar to the apo form, and this maintains an open/flipped out conformation. Furthermore, the 1,3,4-thiadiazole ring interacts with the Met103 side chain, whereas the attached secondary amine can act as a proton donor and forms a H-bond with Met98. By contrast, Tyr158-in inhibitors interact simultaneously with the NADH 2′-hydroxyl group and Tyr158 in a typical H-bond network. Nevertheless, π-stacking interactions with the nicotinamide portion of NADH are present in both types of inhibitors. Shirude *et al.* [50] thus concluded that the essential difference for both of the binding modes is in the nature of the substrate-competitive inhibitors and, in particular, in their overall charge. Thus, the Tyr158-in inhibitors are charged at physiological pH and bind favorably to the NAD^+-bound form of InhA, whereas the Tyr158-out inhibitors are not charged at physiological pH and form additional H-bonds with the hydroxyl group of ribose. Interestingly, when Tyr158 is in the open conformation, access to an additional binding pocket is enabled.

The crystallography of these drug complexes indicated a number of features of InhA that represent valuable resources to guide future efforts in drug design here. In addition, Tyr158-in and Tyr158-out inhibitors have shown antimycobacterial activity *in vitro* and *in vivo*. Therefore, different binding kinetics or different binding modes might ultimately translate into extended residence times on InhA, which will lead to enhanced duration of action.

Concluding remarks

The demanding challenges of continuous and growing TB drug resistance and, unfortunately, the difficulties in translating potent on-target activity into antitubercular activity appear to stand in the way of successful antitubercular drug design. Despite being one of the first antitubercular agents identified, INH remains the most prescribed drug for prophylaxis and TB treatment. Resistance to INH is one of the hallmarks of MDR strains. This article describes how different hit-identification strategies have been applied to InhA as a target for TB, indicating the druggability of the InhA-binding sites via distinct binding mechanisms. The compounds reviewed in this manuscript are InhA inhibitors that have novel binding modes, show solid evidence of successful target engagement and have *in vivo* activity in murine models of TB. For the most recently identified compound (**3**) it has been demonstrated for the first time that it is possible to achieve *in vivo* efficacy comparable with the marketed drug INH using a direct InhA inhibitor. For the foreseeable future, TB will still be treated with multidrug cocktail combinations; however, the emerging data support the concept that a direct inhibitor of InhA is a viable option to obtain novel agents for use in drug combinations in future treatments. We hope that this review will stimulate the research community in industry and academia to target InhA with new drug discovery approaches.

Conflicts of interest

R.Y., A.M. and L.E. are currently employees of GlaxoSmithKline and share stock in the company.

Acknowledgements

This study was supported by the Slovenian Research Agency and the European Union Seventh Framework Programme (FP7/2007-2013) under grant agreement N° 261378. We also thank Chris Berrie for critical reading of the manuscript, and Máire Convery for advice with the X-ray section.

References

1 WHO (2015) *World Health Organisation: Global Tuberculosis Report 2015*. http://www.who.int/tb/publications/global_report/en/
2 WHO (2010) *World Health Organisation: Multidrug and Extensively Drug-Resistant TB (M/XDR-TB): 2010 Global Report on Surveillance and Response*. http://www.who.int/tb/publications/mdr_surveillance/en/
3 CDC (2013) *Centres for Disease Control and Prevention: Managing Drug Interactions in the Treatment of HIV-Related Tuberculosis*. http://www.cdc.gov/tb/publications/guidelines/tb_hiv_drugs/
4 CDC (2003) *Centres for Disease Control and Prevention: Treatment of Tuberculosis*. https://www.cdc.gov/mmwr/preview/mmwrhtml/rr5211a1.htm
5 Wallis, R.S. *et al.* (2016) Tuberculosis advances in development of new drugs, treatment regimens, host-directed therapies, and biomarkers. *Lancet Infect. Dis.* 16, 34–46
6 Quemard, A. *et al.* (1995) Enzymatic characterization of the target for isoniazid in *Mycobacterium tuberculosis*. *Biochemistry* 34, 8235–8241
7 Marrakchi, H. *et al.* (2000) InhA, a target of the antituberculous drug isoniazid, is involved in a mycobacterial fatty acid elongation system, FAS-II. *Microbiology* 146, 289–296
8 Dessen, A. *et al.* (1995) Crystal structure and function of the isoniazid target of *Mycobacterium tuberculosis*. *Science* 267, 1638–1641
9 Bernstein, J. *et al.* (1952) Chemotherapy of experimental tuberculosis. V. Isonicotinic acid hydrazide (nydrazid) and related compounds. *Am. Rev. Tuberc.* 65, 357–364
10 Hazbon, M.H. *et al.* (2006) Population genetics study of isoniazid resistance mutations and evolution of multidrug-resistant *Mycobacterium tuberculosis*. *Antimicrob. Agents Chemother.* 50, 2640–2649
11 Seifert, M. *et al.* (2015) Genetic mutations associated with isoniazid resistance in *Mycobacterium tuberculosis*: a systematic review. *PLOS ONE* 10, e0119628
12 Poce, G. and Biava, M. (2015) Overcoming drug resistance for tuberculosis. *Future Microbiol.* 10, 1735–1741
13 Green, K.D. and Garneau-Tsodikova, S. (2013) Resistance in tuberculosis: what do we know and where can we go? *Front. Microbiol.* 4, 208
14 Lu, X. *et al.* (2011) Enoyl acyl carrier protein reductase inhibitors: a patent review (2006–2010). *Expert Opin. Ther. Pat.* 21, 1007–1022
15 Pan, P. and Tonge, P.J. (2012) Targeting InhA, the FASII enoyl-ACP reductase: SAR studies on novel inhibitor scaffolds. *Curr. Top. Med. Chem.* 12, 672–693
16 Holas, O. *et al.* (2015) *Mycobacterium tuberculosis* enoyl-acyl carrier protein reductase inhibitors as potential antituberculotics: development in the past decade. *J. Enzym. Inhib. Med. Chem.* 30, 629–648
17 Sieniawska, E. (2015) Targeting mycobacterial enzymes with natural products. *Chem. Biol.* 22, 1288–1300
18 Hamid, H. (2016) InhA inhibitors as potential antitubercular agents (a review). *Orient. J. Chem.* 32, 59–75
19 Liu, B. *et al.* (2004) Technological advances in high-throughput screening. *Am. J. Pharmacogenomics* 4, 263–276
20 Mullin, R. (2004) As high-throughput screening draws fire, researchers leverage science to put automation into perspective. *Chem. Eng. News* 82, 23–32
21 Kuo, M.R. *et al.* (2003) Targeting tuberculosis and malaria through inhibition of enoyl reductase. *J. Biol. Chem.* 278, 20851–20859
22 Staveski, M.M. *et al.* (2002) Genzyme Corporation: InhA Inhibitors and Methods of Use Thereof. US6372752 (B1)
23 He, X. *et al.* (2006) Pyrrolidine carboxamides as a novel class of inhibitors of enoyl acyl carrier protein reductase from *Mycobacterium tuberculosis*. *J. Med. Chem.* 49, 6308–6323
24 He, X. *et al.* (2007) Inhibition of the *Mycobacterium tuberculosis* enoyl acyl carrier protein reductase InhA by arylamides. *Bioorg. Med. Chem.* 15, 6649–6658
25 Wall, M.D. *et al.* (2007) Evaluation of *N*-(phenylmethyl)-4-[5-(phenylmethyl)-4,5,6,7-tetrahydro-1H-imidazo[4,5-c]pyridin-4-yl]benzamide inhibitors of *Mycobacterium tuberculosis* growth. *Bioorg. Med. Chem. Lett.* 17, 2740–2744
26 Martínez-Hoyos, M. *et al.* (2016) Antitubercular drugs for an old target: GSK693 as a promising InhA direct inhibitor. *EBioMedicine* 8, 291–301
27 Manjunatha, U.H. *et al.* (2015) Direct inhibitors of InhA are active against *Mycobacterium tuberculosis*. *Sci. Transl. Med.* 7, 269ra3
28 Brenner, S. and Lerner, R.A. (1992) Encoded combinatorial chemistry. *Proc. Natl. Acad. Sci. U. S. A.* 89, 5381–5383
29 Encinas, L. *et al.* (2014) Encoded library technology as a source of hits for the discovery and lead optimization of a potent and selective class of bactericidal direct inhibitors of *Mycobacterium tuberculosis* InhA. *J. Med. Chem.* 57, 1276–1288
30 Frearson, J.A. and Collie, I.T. (2009) HTS and hit finding in academia – from chemical genomics to drug discovery. *Drug Discov. Today* 14, 1150–1158
31 Erlanson, D.A. *et al.* (2016) Twenty years on: the impact of fragments on drug discovery. *Nat. Rev. Drug. Discov.* 15, 605–619
32 Ballell, L. *et al.* (2016) Open Lab as a source of hits and leads against tuberculosis, malaria and kinetoplastid diseases. *Nat. Rev. Drug Discov.* 15, 292–294
33 Schweizer, H.P. (2001) Triclosan: a widely used biocide and its link to antibiotics. *FEMS Microbiol. Lett.* 202, 1–7
34 Sullivan, T.J. *et al.* (2006) High affinity InhA inhibitors with activity against drug-resistant strains of *Mycobacterium tuberculosis*. *ACS Chem. Biol.* 1, 43–53
35 Parikh, S.L. *et al.* (2000) Inhibition of InhA, the enoyl reductase from *Mycobacterium tuberculosis*, by triclosan and isoniazid. *Biochemistry* 39, 7645–7650
36 Luckner, S.R. *et al.* (2010) A slow, tight-binding inhibitor of InhA, the enoyl-acyl carrier protein reductase from *Mycobacterium tuberculosis*. *J. Biol. Chem.* 285, 14330–14337
37 Boyne, M.E. *et al.* (2007) Targeting fatty-acid biosynthesis for the development of novel chemotherapeutics against *Mycobacterium tuberculosis*: evaluation of A-ring-modified diphenyl ethers as high-affinity InhA inhibitors. *Antimicrob. Agents Chemother.* 51, 3562–3567
38 Pan, P. *et al.* (2014) Time-dependent diaryl ether inhibitors of InhA: structure–activity relationship studies of enzyme inhibition, antibacterial activity, and *in-vivo* efficacy. *ChemMedChem* 9, 776–791
39 Li, H.J. *et al.* (2014) A structural and energetic model for the slow-onset inhibition of the *Mycobacterium tuberculosis* enoyl-ACP reductase InhA. *ACS Chem. Biol.* 9, 986–993
40 Lai, C.T. *et al.* (2015) Rational modulation of the induced-fit conformational change for slow-onset inhibition in *Mycobacterium tuberculosis* InhA. *Biochemistry* 54, 4683–4691
41 Wang, H. *et al.* (2015) Radiolabelling and positron emission tomography of PT70, a time-dependent inhibitor of InhA, the *Mycobacterium tuberculosis* enoyl-ACP reductase. *Bioorg. Med. Chem. Lett.* 25, 4782–4786
42 Stec, J. *et al.* (2014) Biological evaluation of potent triclosan-derived inhibitors of the enoyl-acyl carrier protein reductase InhA in drug-sensitive and drug-resistant strains of *Mycobacterium tuberculosis*. *ChemMedChem* 9, 2528–2537
43 am Ende, C.W. *et al.* (2008) Synthesis and *in-vitro* antimycobacterial activity of B-ring modified diaryl ether InhA inhibitors. *Bioorg. Med. Chem. Lett.* 18, 3029–3033
44 Hartkoorn, R.C. *et al.* (2012) Towards a new tuberculosis drug: pyridomycin – nature's isoniazid. *EMBO Mol. Med.* 4, 1032–1042
45 Hartkoorn, R.C. *et al.* (2014) Pyridomycin bridges the NADH- and substrate-binding pockets of the enoyl reductase InhA. *Nat. Chem. Biol.* 10, 96–98
46 Kondreddi, R.R. *et al.* (2014) Pyridone Derivatives and Uses Thereof in the Treatment of Tuberculosis. WO2014093606 A1
47 Ng, P.S. *et al.* (2015) Structure–activity relationships of 4-hydroxy-2-pyridones: a novel class of antituberculosis agents. *Eur. J. Med. Chem.* 106, 144–156
48 Ballell, L.P. *et al.* (2010) Glaxo Group: (Pyrazol-3-yl)-1,3,4-thiadiazol-2-amine and (Pyrazol-3-yl)-1,3,4-thiazol-2-amine compounds. WO2010118852A1
49 Castro, P.J. *et al.* (2012) Glaxo Group: 3-Amino-pyrazole Derivatives Useful Against Tuberculosis. WO2012049161 A1
50 Shirude, P.S. *et al.* (2013) Methyl-thiazoles: a novel mode of inhibition with the potential to develop novel inhibitors targeting InhA in *Mycobacterium tuberculosis*. *J. Med. Chem.* 56, 8533–8542
51 Šink, R. *et al.* (2015) Design, synthesis, and evaluation of new thiadiazole-based direct inhibitors of enoyl acyl carrier protein reductase (InhA) for the treatment of tuberculosis. *J. Med. Chem.* 58, 613–624
52 Rullas, J. *et al.* (2010) Fast standardized therapeutic-efficacy assay for drug discovery against tuberculosis. *Antimicrob. Agents Chemother.* 54, 2262–2264
53 Young, R.J. *et al.* (2011) Getting physical in drug discovery II: the impact of chromatographic hydrophobicity measurements and aromaticity. *Drug Discov. Today* 16, 822–830
54 Rozwarski, D.A. *et al.* (1999) Crystal structure of the *Mycobacterium tuberculosis* enoyl-ACP reductase, InhA, in complex with NAD^+ and a C16 fatty acyl substrate. *J. Biol. Chem.* 274, 15582–15589